

8.3. AQUEOUS CORROSION OF  $U_3O_8$ -AL CERMET CORES

Michelangelo Durazzo and Lalgudi V. Ramanathan,  
Instituto de Pesquisas Energéticas e Nucleares  
São Paulo, Brazil

## ABSTRACT

Materials Testing of Reactor type fuel elements containing fuel plates with  $U_3O_8$ -Al cermet cores are being developed at the Nuclear and Energy Research Institute, São Paulo, Brazil, and apart of the programme involves the corrosion characterization of the fuel plate cermet cores. Fuel plate specimens containing (a) cores with varying concentrations of natural  $U_3O_8$  and (b) cores from compacts with different densities, were fabricated and their corrosion behaviour were tested by exposing the cermet core through an artificial defect in the cladding to deionized water at 30, 50, 70 and 90°C. The results obtained revealed that core corrosion was accompanied by hydrogen evolution. The total volume of hydrogen evolved (V) and the time to initiation of hydrogen evolution ( $t_i$ ) have been found to vary with porosity in the cermet core and with temperature according to:

$$V = K_1 \exp(\alpha_1 P) - K_2 \cdot T \exp(\alpha_2 P) \text{ and } t_i = \exp(K_1 + K_2 \cdot P + K_3/T + K_4 \cdot P/T) \text{ where } P \text{ is the volumetric pore fraction}$$

and  $k_1, k_2, k_3, k_4, \alpha_1$  and  $\alpha_2$  are constants. A mechanism to explain the cermet core corrosion has been proposed and discussed.

## INTRODUCTION

Recent emphasis to reduce the risk of diversion of highly enriched uranium (containing ~93%  $U^{235}$ ) for non-peaceful purposes has curtailed its commercialisation, and has led to an impetus for reducing the enrichment level of fuels for research and test reactors to low enriched uranium (~20%  $U^{235}$ ). One of the main programmes at the Department of Nuclear Metallurgy of the Instituto de Pesquisas Energéticas e Nucleares (Energy and Nuclear Research Institute), São Paulo, has been the development of fabrication procedures for M.T.R. (Materials Testing Reactor) type fuel elements containing low enriched  $U_3O_8$ -Al cermet cores, for its swimming pool type research reactor IEA-R1. Part of the programme was to study the aqueous corrosion behavior of  $U_3O_8$ -Al



cermet cores under simulated conditions of cladding rupture in service.

Literature survey revealed very little information about  $U_3O_8$ -Al cermet corrosion. Stahl [ 1 ] reported that when fuel plates containing  $U_3O_8$ -Al and  $U_3Si$ -Al cores were exposed to boiling demineralized water, through an artificially created cladding defect, there was no fuel loss or fuel plate swelling after 168 hours.

Kucera [ 2 ] also studied the corrosion of  $U_3O_8$ -Al fuel plate cores by exposing them for 25 weeks to high purity water at  $90^{\circ}C$  through an artificially created cladding defect, and reported that the core corrosion resistance was satisfactory. However, preliminary investigations carried out by the authors, with fuel plate specimens containing  $U_3O_8$ -Al cermet cores, revealed that upon exposing the core to water, appreciable quantities of hydrogen was evolved, (up to 2000 ml in 200 minutes at  $50^{\circ}C$ ) [ 3 ]. The evolution of hydrogen from a fuel element poses another serious problem: that of reactor safety, as the hydrogen can act as a possible carrier for gaseous fission products. Hence, to throw more light on the corrosion behavior of exposed  $U_3O_8$ -Al cermet cores, the influence of core composition, core density and water temperature on hydrogen evolution behavior was investigated and the results are presented in this paper.

#### EXPERIMENTAL

The  $U_3O_8$ -Al cermet compact preparation procedure is shown schematically in figure 1. The compacts were subsequently

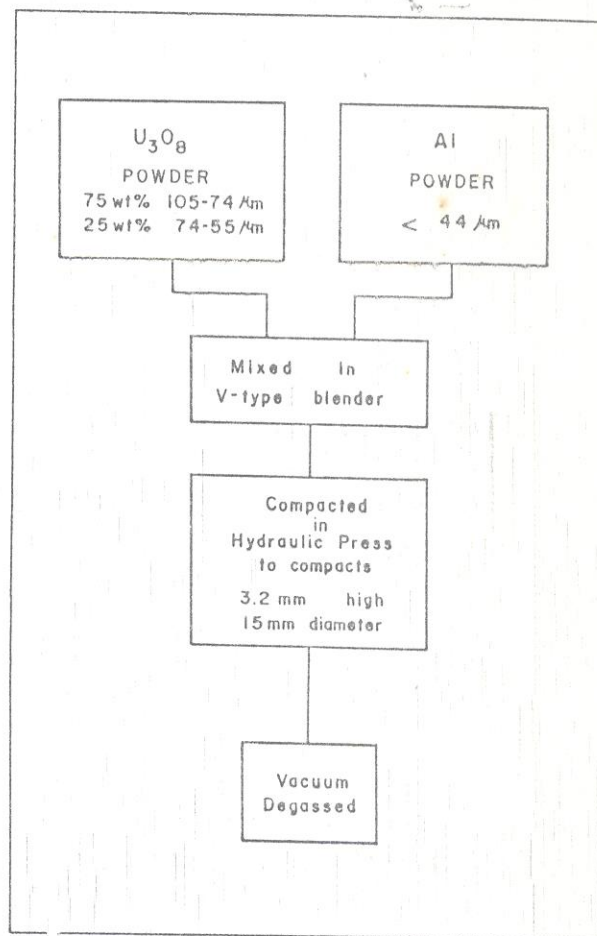


FIGURE 1 -  $U_3O_8$ -Al cermet compact preparation procedure.

positioned in Al-1100 frames as shown in figure 2, welded, hotrolled, tested for blisters and cold-rolled to obtain plates 1 mm thick [ 4,5 ]. The total reduction in thickness was 89.5%. The plates were then radiographed to locate the cores and, the fuel plate specimens cut out. The density of the core was determined hydrostatically with water as the liquid.

Two sets of fuel plate specimens were made. In the first, the cermet composition was maintained constant at 58 wt% natural  $U_3O_8$ , 42 wt% Al, and the starting density of the powder compact varied to



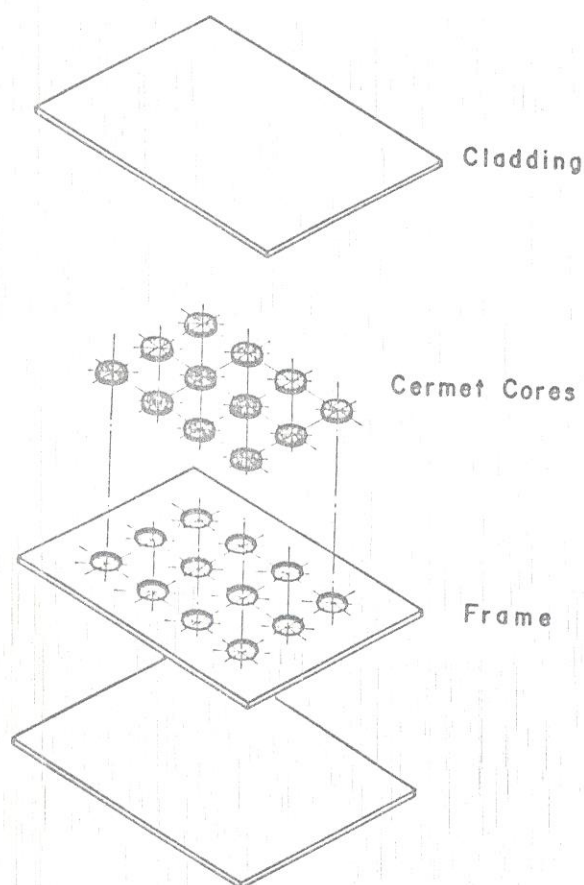


FIGURE 2 - Schematic arrangement of cladding plates, frame and cermet cores prior to assembly.

be at 75, 80, 85, 90 and 95% of its theoretical density. In the second set, the cermet core composition was varied to give specimens containing 10, 20, 30, 40, 50, 58, 70, 75, 80, 85 and 90 wt%  $U_3O_8$ , but the powder compact density was maintained constant at 85% of its theoretical density.

#### Corrosion tests.

Corrosion of the  $U_3O_8$ -Al cores was

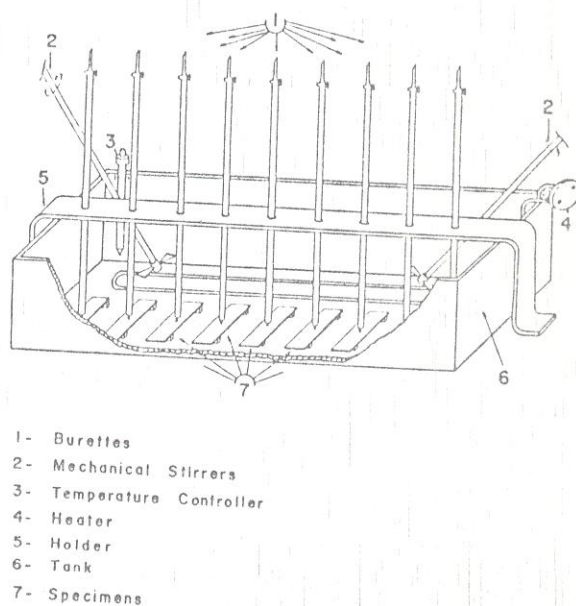


FIGURE 3 - Schematic view of experimental setup for conducting corrosion tests.

evaluated through measurements of the volume of hydrogen evolved when the cores were exposed to deionized water. The experimental set up for the corrosion tests is shown in figure 3. The fuel plate specimens were drilled under deionized water in a polypropylene tank 1m x 0.4m x 0.25m, to simulate a cladding defect. Water filled burettes positioned vertically over and 5mm away from the drilled hole enabled collection and direct measurement of the hydrogen evolved. The water temperature was controlled to an accuracy of  $1^{\circ}C$  and kept homogeneous with the aid of stainless steel stirrers. The tests were carried out at 30, 50, 70 and  $90^{\circ}C$ , to cover the complete range of operating temperatures of the IEA-R1 reactor. Three specimens cor-



responding to each cermet composition and cermet density were tested at each of the temperatures. The specimens were drilled ( $0.8\text{mm } \varnothing$ ), about ten minutes after introduction into the tank, to allow for temperature equilibration. The volume of hydrogen evolved was periodically read and the curves of volume of hydrogen versus time were plotted. The water resistivity varied between  $0.7 \times 10^6 \Omega \cdot \text{cm}$  (at the beginning of the test) and  $0.1 \times 10^6 \Omega \cdot \text{cm}$  (at the end of the test), and the pH between 5.8 and 5.2.

## RESULTS AND DISCUSSIONS

Figures 4 and 5 show the influence of  $\text{U}_3\text{O}_8$  concentration in the fuel plate core, and the influence of water temperature, respectively, on hydrogen evolution as a function of time. The hydrogen evolution curves are characterized by an initial incubation period during which no hydrogen evolution takes place, a second period during which hydrogen evolution takes place

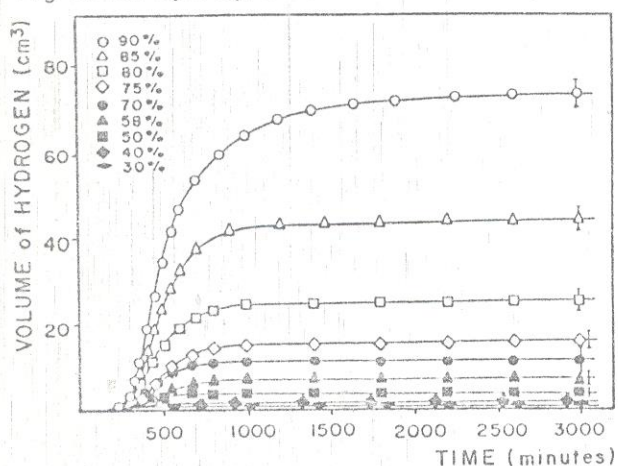


FIGURE 4 - Curves of  $\text{H}_2$  evolution from cores with varying concentration of  $\text{U}_3\text{O}_8$ .

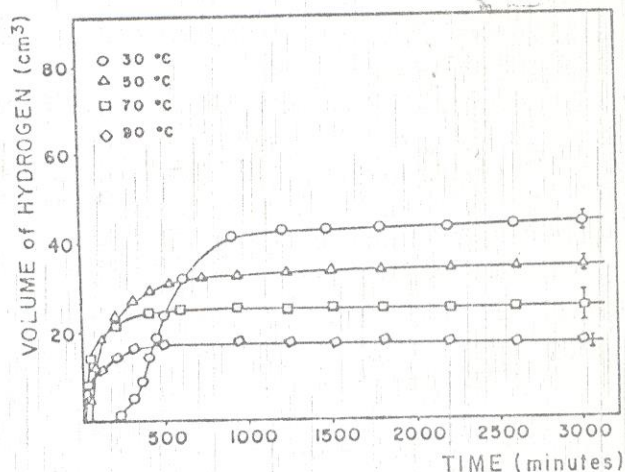


FIGURE 5 - Curves of  $\text{H}_2$  evolution from cores with 85 wt%  $\text{U}_3\text{O}_8$  at different temperatures.

at an increasing rate, and after having reached a maximum, reduces to a very low rate or ceases. The sigmoidal form of the curves, especially at low temperatures ( $30^\circ\text{C}$ ) indicates that the reaction between the  $\text{U}_3\text{O}_8$ -Al core and water is possibly autocatalytic. The total volume of hydrogen evolved ( $V$ ) (hydrogen evolved in 3000 minutes and corresponding to the plateau of the curve), as well as the incubation time ( $t_i$ ), considered to be the time before the first hydrogen bubble was observed, are the two main and relevant parameters in terms of the core corrosion process. It can be seen from figures 4 and 5 that  $V$  depends on the concentration of  $\text{U}_3\text{O}_8$  in the core and the water temperature. An increase in the concentration of  $\text{U}_3\text{O}_8$  or a decrease in temperature, increases  $V$ . Hydrogen evolution was not observed from specimens with low  $\text{U}_3\text{O}_8$  con-



centrations (up to 20 wt% at 30°C, up to 40 wt% at 50°C and up to 50 wt%  $U_3O_8$  at 70°C). The incubation time  $t_i$  on the other hand is more sensitive to changes in temperature than to changes in  $U_3O_8$  concentration.

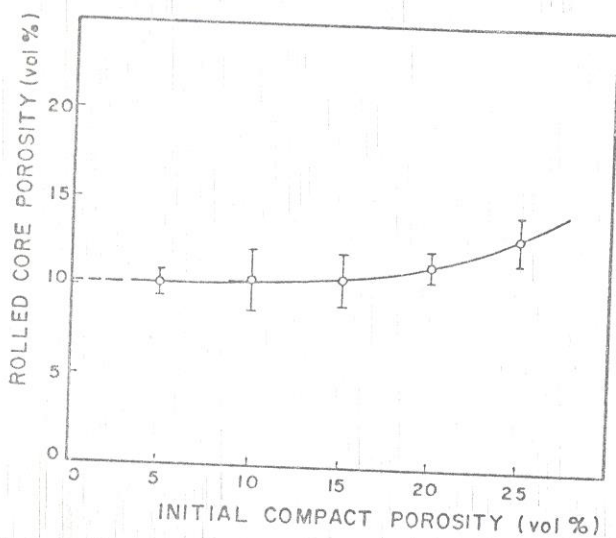


FIGURE 6 - Effect of initial cermet compact porosity on final rolled core porosity.

Figure 6 shows the effect of porosity in the initial cermet compact on the final rolled core porosity. It can be seen that changes in porosity in the cermet compact for a specific  $U_3O_8$  concentration do not influence the porosity in the rolled core; and the latter attains an equilibrium value. The shift from equilibrium porosity in the case of cores with high initial compact porosity can be attributed to the introduction of irregularities in the core, during the first few passes in the rolling mill.

On the other hand, an increase in  $U_3O_8$  concentration increases porosity in the rolled core, as shown in figure 7. At  $U_3O_8$  concentrations between 70 and 80 wt%

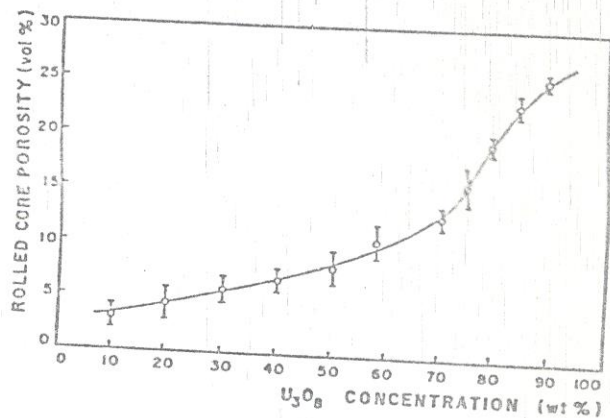


FIGURE 7 - Effect of  $U_3O_8$  concentration on porosity in rolled core.

the porosity in the rolled core increases markedly. The effect of  $U_3O_8$  concentration on the total volume of hydrogen evolved  $V$  at various temperatures is shown in figure 8. Once again, a marked increase in  $V$  from specimens with 70-80 wt%  $U_3O_8$  can be observed. This indicates that  $V$  is prima-

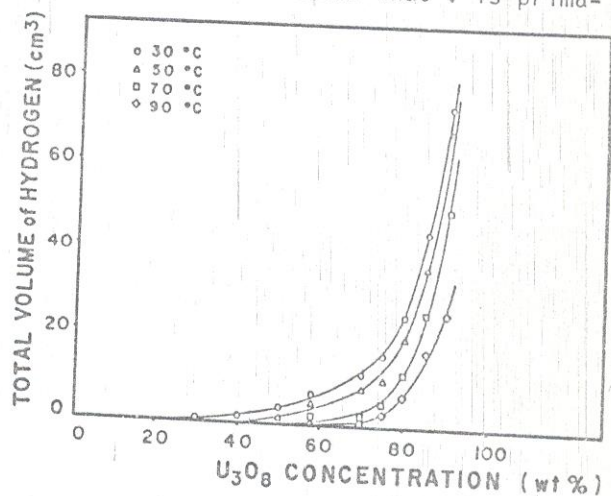


FIGURE 8 - Effect of  $U_3O_8$  concentration on total volume of hydrogen evolved.

rially dependent on the equilibrium porosity of the rolled core, which in turn depends



on the  $U_3O_8$  concentration, its resistance to fragmentation as well as the rolling conditions. Furthermore, it can be seen from micrographs shown in figure 9 that the nature of the pores present in the

core permit easy ingress of water into the interior of the core, away from the drilled hole, affecting thus the total volume of hydrogen evolved.

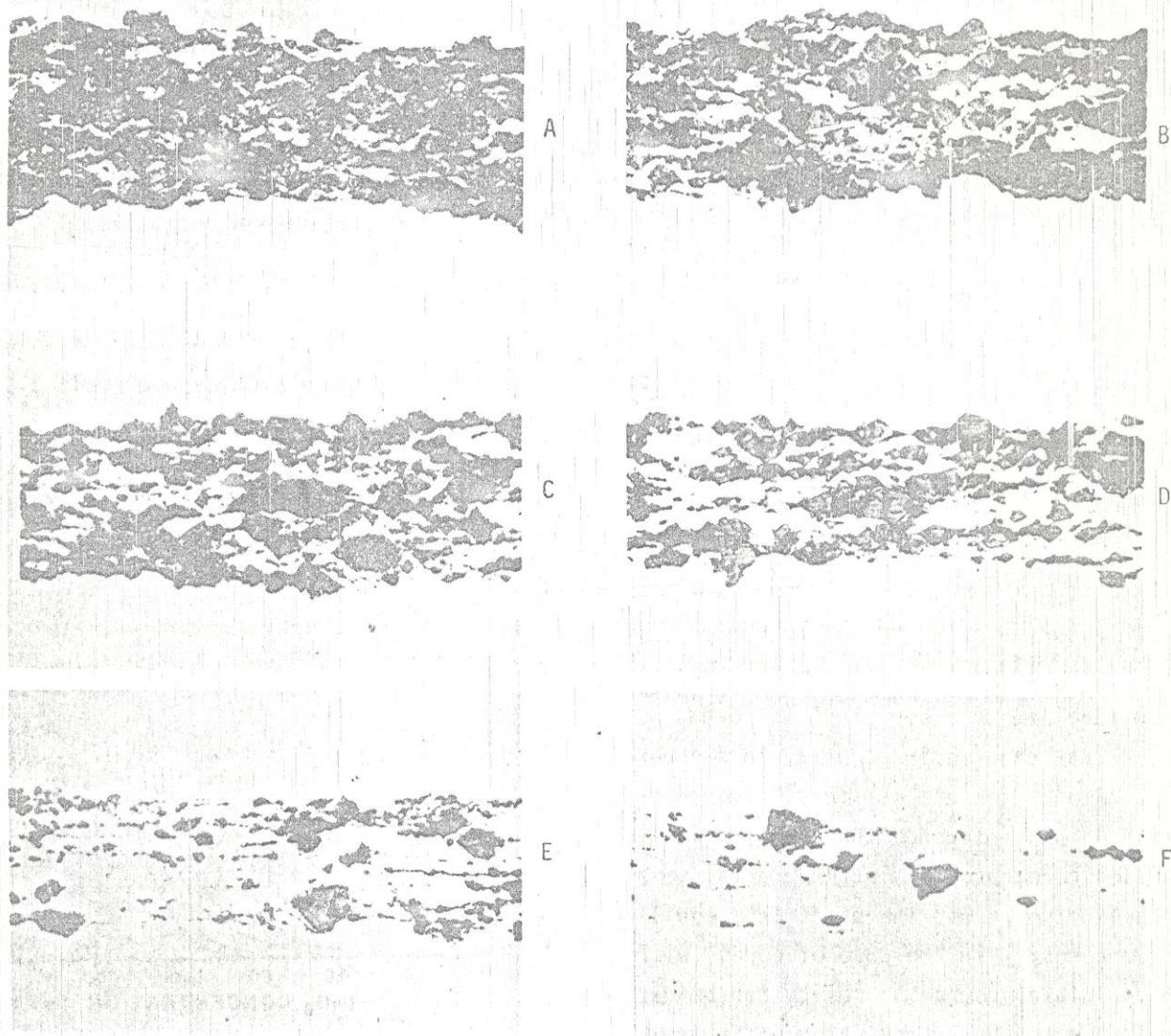


FIGURE 9 - Micrographs of longitudinal sections of  $U_3O_8$ -Al cermet cores containing varying concentrations of  $U_3O_8$ . No etchant was used and equilibrium porosity values are shown. Magnification-80 X.

A - 90 wt%  $U_3O_8$ -25.44 vol% pores  
C - 75 wt%  $U_3O_8$ -15.81 vol% pores  
E - 50 wt%  $U_3O_8$ - 8.14 vol% pores

B - 80 wt%  $U_3O_8$ -19.56 vol% pores  
D - 70 wt%  $U_3O_8$ -12.37 vol% pores  
F - 30 wt%  $U_3O_8$ - 5.83 vol% pores



Using non-linear multiple regression analysis the experimental results were fitted to equations 1 and 2 for  $V$  and  $t_i$  respectively, as functions of the volumetric pore fraction  $P$  and the water temperature  $T$  (K):

$$V = K_1 \cdot \exp(\alpha_1 \cdot P) - K_2 \cdot T \cdot \exp(\alpha_2 \cdot P) \quad (1)$$

$$t_i = \exp(K_1 + K_2 \cdot P + K_3/T + K_4 \cdot P/T) \quad (2)$$

where  $K_1$ ,  $K_2$ ,  $K_3$ ,  $K_4$ ,  $\alpha_1$  and  $\alpha_2$  are constants. From equation 1 it can be seen that at constant temperature,  $V$  varies as a function of porosity and can be expressed as two exponentials. Similarly with porosity maintained constant,  $V$  varies linearly with temperature.

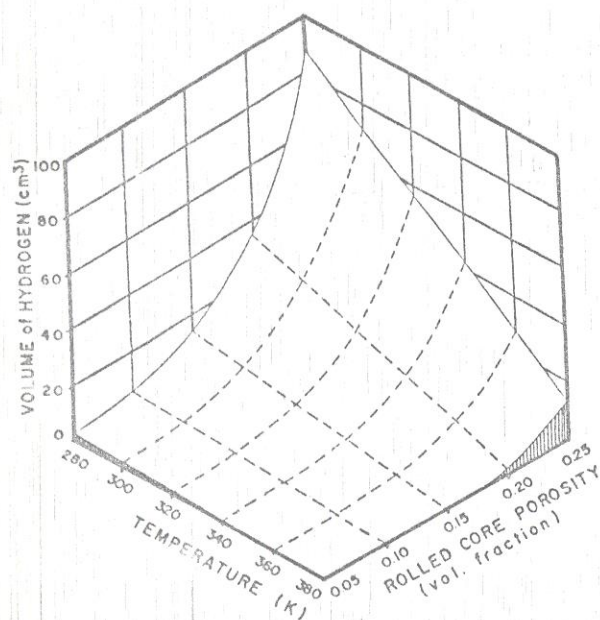


FIGURE 10 - Regression surface representative of equation 1.

Figure 10 shows the regression surface obtained upon fitting the experimental results to equation 1. The values for  $K_1$ ,

$K_2$ ,  $\alpha_1$  and  $\alpha_2$  as well as the correlation coefficient are given in Table I.

Constants	values
$K_1$	4.3801
$K_2$	0.0127
$\alpha_1$	16.8054
$\alpha_2$	16.2263

Correlation Coefficient = 0.9834

TABLE I - Values of constants for fitting experimental values to equation 1.

Equation 2 shows that at constant porosity,  $t_i$  varies exponentially with the inverse of absolute temperature and at constant temperature,  $t_i$  again varies exponentially with porosity. Figure 11 shows the regression surface obtained upon fitting the experimental results to equation 2, and Table II lists the values for constants  $K_1$ ,  $K_2$ ,  $K_3$  and  $K_4$  and the correlation coefficient.

#### Mechanism

The nature of hydrogen evolution curves suggests that when the cladding is ruptured and the  $U_3O_8$ -Al core is exposed, water enters rapidly through the channels (elongated gaps along the rolling direction - vide figure 9) present in the core and reacts with the aluminium in the core. These channels formed during the rolling operation are free of any gas or vapour and facilitate easy ingress for water. Once inside the core, the water rapidly reacts with the film free aluminium surfaces and forms a protective surface film of aluminium



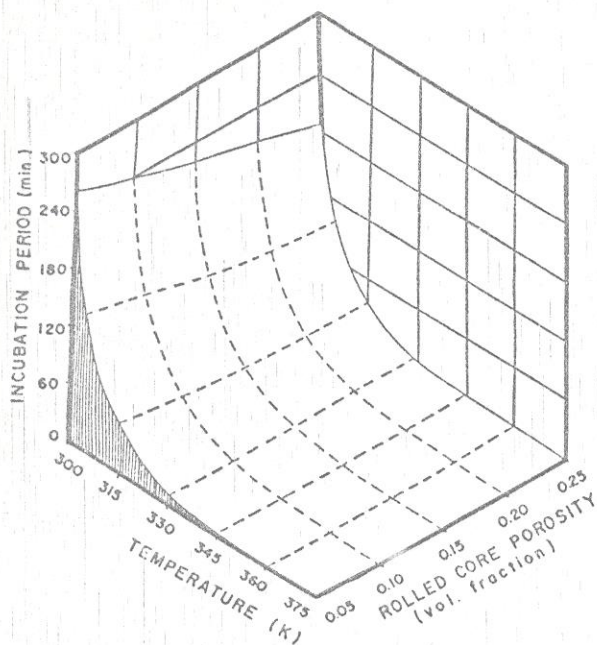


FIGURE 11 - Regression surface representative of equation 2.

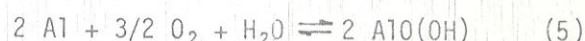
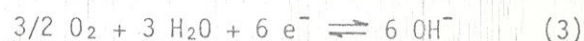
Constants	values
$K_1$	-27.3825
$K_2$	-21.8726
$K_3$	9907.7355
$K_4$	6060.0316

Correlation Coefficient = 0.9918

TABLE II - Values of constants for fitting experimental values to equation 2.

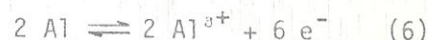
um oxide, possibly amorphous alumina and/or boehmite; oxides typically formed during the initial stages of corrosion of aluminium at low temperatures [6-8]. After the initial rapid reaction, the oxide layer prob-

ably grows logarithmically with time [8,9] till all the dissolved oxygen available in the interior of the cermet core is consumed in the cathodic oxygen reduction reaction (typical cathodic reaction in neutral oxygen containing solution) according to:



or  
 $Al_2O_3 \cdot H_2O$   
 (Boehmite)

Soon after, with no more dissolved oxygen available inside the core, the oxygen reduction reaction shifts to the cladding surface outside the core crevice, where dissolved oxygen continues to be available and the anodic reaction shown in equations 6 and 7 continue to take place inside the core.



This causes a localized lowering of pH in the core and gives rise to two effects: (a) The hydrogen evolution reaction taking place inside the core according to:



(characteristic cathodic reaction in low pH solutions in the absence of dissolved oxygen) and (b) Dissolution of the oxide layer present on the aluminium surfaces inside the core [10], followed by an increase



in aluminium corrosion rate and a consequent increase in the rate of hydrogen evolution. The increase in aluminium corrosion rate within the core leads to an increase in  $H^+$  concentration, lowering of pH even more, a consequent increase in rate of oxide dissolution and a further increase in the rate of aluminium corrosion and hydrogen evolution, characterizing an autocatalytic process. The rate of hydrogen evolution thus attains a maximum value. After a certain time, the aluminium ion concentration in the solution within the core increases to levels when further dissolution is inhibited [11-13] and accordingly the rates of both aluminium dissolution and hydrogen evolution.

An increase in porosity within the core implies an increase in the total area of aluminium within the core, which upon exposure to water results in an increase in the total volume of hydrogen evolved. Also, in specimens with high core porosity, the presence of longer and interlinked channels facilitates penetration of the water to greater distances, away from the artificially created cladding defect and results in the liberation of a greater volume of hydrogen. Decrease in  $V$  with increasing water temperature may be attributed to formation of more stable boehmite at higher temperatures [6,14] which inhibits aluminium corrosion. The exponential decrease in  $t_i$  with increasing temperature may be attributed to the increased rate with which the initial stages of core corrosion take place. Decrease in  $t_i$  with cermet porosity is due to the evolution of large quantities of hydrogen which increase gas pressure within

the core crevices and bring forward the appearance of the first hydrogen bubble.

## CONCLUSIONS

1. In the case of cladding failure of fuel plates containing  $U_3O_8$ -Al cermet cores, the corrosion of the core is accompanied by hydrogen evolution. The hydrogen evolution process is characterized by an incubation period followed by a period when the hydrogen evolution rate increases and reaches a maximum, and a period when it decreases till hydrogen evolution ceases.
2. The two main parameters relevant to the  $U_3O_8$ -Al cermet core corrosion process are the total volume of hydrogen evolved  $V$  and the incubation period  $t_i$ .
3. The volume of hydrogen evolved is independent of the starting compact porosity and depends on the porosity of the plate core  $P$  and water temperature  $T$  (K) according to:  

$$V = K_1 \cdot \exp(\alpha_1 \cdot P) - K_2 \cdot \exp(\alpha_2 \cdot P)$$

$$t_i = \exp(K_1 + K_2 \cdot P + K_3/T + K_4 \cdot P/T)$$
 where  $K_1$ ,  $K_2$ ,  $K_3$ ,  $K_4$ ,  $\alpha_1$  and  $\alpha_2$  are constants.
4. Data about the total volume of hydrogen evolved from corrosion of  $U_3O_8$ -Al cores and the incubation periods could complement safety studies in the operation of swimming pool type reactors using M.T.R. type plate fuels.



# REFERENCES

1. - D. STAHL., Argonne National Lab.,  
Argonne, Ill., ANL-83-5, 1982.
2. - W.J. KUCERA., Oak Ridge National Lab.,  
Oak Ridge, Tn., ORNL-2839, 1959.
3. - J.C. BRESSIANI, M. DURAZZO,  
L.V. RAMANATHAN and C.T. FREITAS.  
Proc. 35th Ann. Conf. Brazilian  
Association for Metals, São Paulo,  
Brazil, July, 1980, 597.
4. - T.D. SOUZA SANTOS, H.M. HAYDT and  
C.T. FREITAS. Metalurgia (Brazil),  
21, (1965), 369.
5. - A.R. KAUFMAN., Nuclear Reactor Fuel  
Elements - Metallurgy and Fabrication,  
Interscience, N.Y., (1962).
6. - R.K. HART., Trans. Faraday Soc., 53,  
(1957), 1020.
7. - J.E. DRALEY and W.E. RUTHER.,  
Corrosion, 12, (1956), 441t.
8. - M. KAWASAKI, S. NOMURA, H. ITAMI,  
Y. KONDO, T. KONDO, N. ITU and  
C. AKUTSU. Conference on Corrosion  
of Reactor Materials, Salzburg,  
Austria, June 1962. 427.
9. - J.E. DRALEY., Conference on Corrosion  
of Nuclear Materials, Brussels,  
Belgium, October 1959, 165 .  
(TID 7587).
10. - V.H. TROUTNER. Hanford Atomic Pro-  
ducts Operations, Richland, Wa.,  
HW-50133, 1957.
11. - K. VIDEM. J. Nucl. Mater. 2, (1959),  
145.
12. - R.J. LOBSINGER. Hanford Atomic Pro-  
ducts Operations, Richland, Wa.,  
HW-59778 Rev., 1961.
13. - J.E. DRALEY, C.R. BREDEN, W.E. RUTHER  
and N.R. GRANT. Conference on  
Peaceful Uses of Atomic Energy,  
Geneva, September 1958, V.5, 113.
14. - R.S. ALWITT and L.C. ARCHIBALD.  
Corrosion Sci. 13 (1973) 687.